Available online at www.sciencedirect.com
ScienceDirect
Journal of Chromatography B, 848 (2007) 200–207
JOURNAL OF CHROMATOGRAPHY B
www.elsevier.com/locate/chromb

A capillary-based microfluidic instrument suitable for immunoaffinity chromatography

Michael C. Peoples [a], Terry M. Phillips [b], H. Thomas Karnes [a,*]

[a] *Department of Pharmaceutics, Virginia Commonwealth University Medical Center, P.O. Box 980533, Richmond, VA 23298-0533, United States*
[b] *Ultramicro Analytical Immunochemistry Resource, Division of Bioengineering and Physical Science, Office of Research Services, National Institutes of Health, 9000 Rockville Pike, Bethesda, MD 20892, United States*

Received 26 June 2006; accepted 16 October 2006
Available online 13 November 2006

Abstract

The analysis of biological samples to produce clinical or research data often requires measurement of analytes from complex biological matrices and limited volumes. Miniaturized analytical systems capable of minimal sample consumption and reduced analysis times have been employed to meet this need. The small footprint of this technology offers the potential for portability and patient point-of-care testing. A prototype microfluidic system has been developed and is presented for potential rapid assessment of clinical samples. The system has been designed for immunoaffinity chromatography as a means of separating analytes of interest from biological matrices. The instrument is capable of sub-microliter sample injection and detection of labeled antigens by long wavelength laser-induced fluorescence (LIF). The laboratory-constructed device is assembled from an array of components including two syringe pumps, a nano-gradient mixing chip, a micro-injector, a diode laser, and a separation capillary column made from a polymer/silica (PEEKsil) tube. An in-house program written with LabVIEW software controls the syringe pumps to perform step gradient elution and collects the LIF signal as a chromatogram. Initial columns were packed with silica beads to evaluate the system. Optimization of the device has been achieved by measuring flow accuracy with respect to column length and particle size. Syringe size and pressure effects have also been used to characterize the capability of the pumps. Based on test results, a 200-μm × 25-mm column packed with 1-μm silica beads was chosen for use with a 500-μL syringe. The system was tested for mixer proportioning by pumping different compositions of buffer and fluorescent dye solutions in a stepwise fashion. A linear response was achieved for increasing concentrations of fluorescent dye by online mixing ($R^2 = 0.9998$). The effectiveness of an acidic gradient was confirmed by monitoring pH post-column and measuring premixed solutions offline. Finally, assessment of detectability was achieved by injecting fluorescent dye solutions and measuring the signal from the LIF detector. The limit of detection for the system with these solutions was 10.0 pM or 10.0 amol on-column. As proof-of-principle, immunoaffinity chromatography was demonstrated with immobilized rabbit anti-goat IgG and a fluorescent dye-goat IgG conjugate as a model antigen.

Keywords: Microfluidics; Immunoglobulins; Immunoaffinity; Laser induced fluorescence; Capillary chromatography

1. Introduction

The analysis of complex biological sample matrices for clinical and research purposes requires the use of selective analytical technology for measurement of target analytes. Additionally, limited sample quantities and the potential need for patient point-of-care testing have necessitated the development of miniaturized instrumentation and microfluidic devices [1]. Immunoaffinity separation techniques, capable of isolating specific analytes by formation of an antibody–antigen complex, have been applied in a variety of formats suitable for small-scale bioanalysis. Immunoassay-based solid phase supports have been used for sample extraction and purification prior to a secondary separation step, such as chromatography or capillary electrophoresis [2–5]. Immunoaffinity extraction can provide greater selectivity than traditional solid phase extraction supports due to the nature of the antibody–antigen binding [2]. Immunoassays and immunoaffinity separations have been presented in several miniaturized systems, including microchips and capillary-based instruments. Microfluidic chips may involve electroosmotic or hydrodynamic pumping for fluid control with immunoaffinity separation in open or packed channels, and

* Corresponding author. Tel.: +1 804 828 3819; fax: +1 804 828 8359.
E-mail address: tom.karnes@vcu.edu (H.T. Karnes).

1570-0232/$ – see front matter © 2006 Elsevier B.V. All rights reserved.
doi:10.1016/j.jchromb.2006.10.032

several platforms have been demonstrated [6–14]. Immunoaffinity capillary electrophoresis has been demonstrated for single and multiple analyte analyses in fused-silica capillaries [15,16]. Immunoaffinity chromatographic systems and flow immunoassays have been employed as well, with micro-separations occurring in capillary columns or channels [17–19]. Several reviews and reports have been recently published on immunoextraction sample preparation, immunoaffinity capillary electrophoresis, and immunoaffinity chromatography [2,3,20–24].

Immunoaffinity chromatography systems for micro-scale separations involve the use of pumps to force fluids through capillaries and channels either open or packed with solid particles, such as beads. Pumps capable of μL/min flow rates are often required and peristaltic or syringe pumps have been used. Bead-based immunoassays using immobilized antibodies have been used for qualitative and quantitative biomedical analysis [25]. Beads may also be utilized as solid supports to attach antibodies for immunoaffinity stationary phases. Separation capillaries packed with beads offer the advantage of reduced diffusion distances for mass transport and the ability to concentrate samples online in a fluidic system over open tubular capillaries [26,27]. Antibody-coated bead supports also create reduced interstitial volumes for antibody–antigen recognition. Sample antigen may be loaded onto and captured by immobilized antibody beads and released in a reduced volume, thereby enhancing the signal.

A number of different supports including magnetic, plastic, glass, and silica beads as well as monolithic supports have been applied for immunoaffinity chromatography. A magnetic bead-based flow immunoassay was demonstrated in both microchannel and capillary formats for sandwich immunoassays of parathyroid hormone and interleukin-5 [19]. A glass bead direct capture immunoaffinity separation of substance P in multiple biological sample matrices was achieved with a liquid chromatography system made from microdialysis pumps and a fused-silica separation capillary [18]. Polystyrene antibody-coated beads packed into chip-based microchannels have been employed for analysis of human carcinoembryonic antigen and Tacrolimus in separate studies [8,13]. Capillary columns made from monolithic supports containing stationary antibodies were prepared and tested using fluorescein as a model antigen [28]. Monolithic disks for immunoaffinity extraction were reported for rapid isolation of rabbit IgG and fluorescein models [29].

Syringe pumps or conventional HPLC pumps with unique mixers have been employed to produce gradients for capillary liquid chromatography and microfluidic devices because of their commercial availability and ease of use. Ducret et al. [30] reported the use of two syringe pumps to produce gradients for capillary HPLC with electrospray ionization mass spectrometry. A capillary mixing chamber was constructed using capillary tubing and a steel ball from a ball point pen. Cappiello et al. [31] described the use of a 14-port switching valve and flow-splitting with conventional HPLC pumps to produce nano- and microflow gradients. The switching valve metered mobile phase mixtures from six pre-filled loops for gradient generation. Zhou et al. [32] demonstrated gradient mixing for capillary HPLC with mass spectrometric detection using a single syringe pump and a micro-autosampler. The autosampler was used to generate gradients by injecting programmed volumes of premixed mobile phase solutions from separate vials.

The aim of this work is to design a capillary HPLC system suitable for performing immunoaffinity chromatography separations in biological samples. The system was developed for small volume sample injection with the ability to detect fluorescent laser dye conjugates in the picomolar (pM) range. Additionally, many of the system components are commercially-available and reasonably straightforward to assemble. Two syringe pumps were programmed together in an original format for microfluidic step gradient elution and a detailed design is included for assembly of a capillary scale separation column. The laboratory-built instrumentation and software program are presented here, along with initial results of an immunoaffinity separation as proof-of-principle.

2. Experimental

2.1. Reagents and materials

Plain 1 μm silica beads were purchased from Polysciences (Warrington, PA). Alexa Fluor 647 succinimidyl dye (λ_{ex} = 650 nm, λ_{em} = 670 nm) was obtained from Invitrogen (Carlsbad, CA). Streptavidin-coated 5.7 μm glass particles were purchased from Xenopore (Hawthorne, NJ). Biotin-conjugated polyclonal rabbit anti-goat IgG (H + L) and Alexa Fluor 647-conjugated polyclonal goat IgG (anti-human) were obtained from Invitrogen. Purified water was made in-house using a Barnstead Nanopure Diamond system (Dubuque, IW). All other chemicals were purchased from Sigma (St. Louis, MO).

2.2. Instrumentation

The basic components of the instrumentation are shown in Fig. 1. Dual microliter OEM module syringe pumps from Harvard Apparatus Inc. (Holliston, MA) were mounted side-by-side in a 0.22 in. clear acrylic housing. Twin LCD display chips were wired to the pump boards to allow for confirmation of power up and flow rate. Glass gastight 1700 series syringes with 22-gauge blunt needle tips (Hamilton, Reno, NV) were used with the pumps. Each syringe needle tip was connected by a union to a length of 360 μm outer diameter (o.d.) × 100 μm inner diameter (i.d.) polyetheretherketone (PEEK) capillary tubing (Upchurch Scientific, Oak Harbor, WA). The PEEK capillary was attached to a nano-scale mixer (NanoMixer, Upchurch Scientific) mounted on the front of the pump cabinet enclosure. The NanoMixer is a gradient mixing chip capable of low and high mixing configurations, requiring 30 and 60 nL of fluid, respectively. The mixer was connected by a single length of 100 μm i.d. PEEK capillary to one of six ports of a Microinjector (Upchurch Scientific). Injection loops were made with capillary PEEK tubing by treating the tubing as a cylinder and cutting the capillary to the appropriate length based on the calculated volume.

A 20 mW 650-nm laser diode (Lasermate Group Inc., Pomona, CA) was housed in a LDM 4412 laser diode mount (ILX Lightwave, Bozeman, MT) with a collimating lens. Thermoelectric cooling and current control were maintained by an

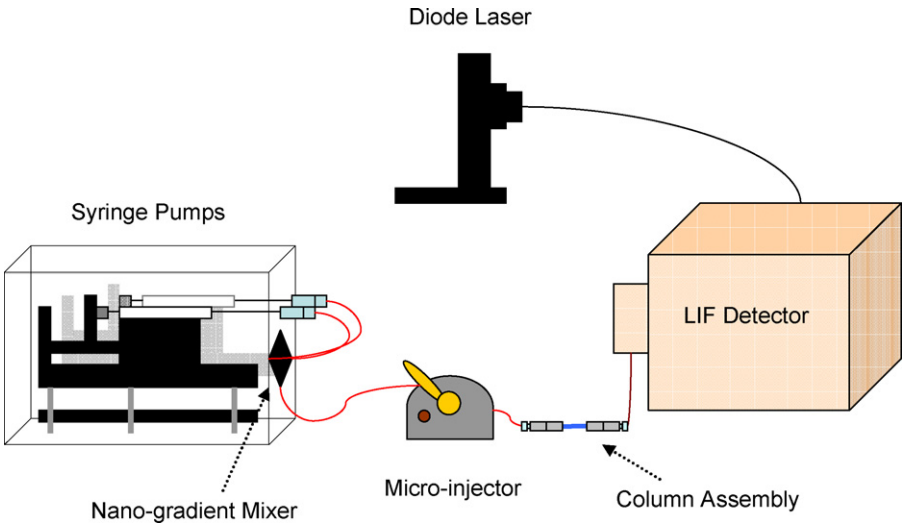

Fig. 1. Diagram of capillary LC with laser-induced fluorescence detection.

ILX Lightwave model LDC-3722 laser diode controller (20 °C; 60 mA). Output power and wavelength were measured with a model OMM-6810B optical multimeter (ILX Lightwave). The laser was operated at a typical power output of 16 mW measured at the optical bench. The front of the laser diode module was attached to a fiber optic that was connected to a Zetalif laser-induced fluorescence detector (Picometrics, Ramonville, France). The laser light in the Zetalif detector is brought to a dichroic mirror and reflected onto a 2 mm ball lens. The excitation beam is focused onto a capillary flow cell and fluorescence is collected back through the ball lens in a collinear arrangement. High pass, spatial, and notch filters (Omega Optical Inc., Brattleboro, VT) were placed in the light path before the emitted light hits a Hamamatsu model R928 red-sensitive photomultiplier tube (Bridgeport, NJ). The photomultiplier tube was routinely operated at 700 V. The flow cell was made from square fused silica capillary tubing with dimensions of 360 μm o.d. by 100 μm i.d. (Polymicro Technologies, Phoenix, AZ). A 2 mm detection window was created by burning off the polyimide coating with a capillary window maker (MicoSolv Technology Corporation, Long Branch, NJ). The detector signal was introduced to a computer via a National Instruments USB-9215 data acquisition card with 16-bit resolution (Austin, TX).

2.3. Column design

Prototype columns were constructed from PEEKsil tubing (Upchurch) with dimensions of 200 μm i.d. × 1/16 in. o.d. Stainless steel external column endfittings and ferrules were purchased from Valco Instrument Co. Inc. (Houston, TX). A stainless steel 0.5 μm frit with polymer ring (Upchurch) and dimensions 0.038 in. × 0.030 in. × 0.062 in. was used to retain stationary phase material. PEEKsil is polyetheretherketone-coated capillary tubing with a fused-silica inner core. The polymer outer layer adds protection and rigidity to the fused silica and the material is rated at a pressure of 8500 psi. The tubing ends are machine cut and level, making them suitable for chromatography columns. The endfittings were wrench-tightened onto the columns with frits attached to set the ferrules. One endfitting assembly and one frit were removed to allow for packing. A detailed view of the column components is shown in Fig. 2.

Columns were packed under negative pressure (approximately 600 psi maximum) using a vacuum pump and adding a 3 mg/mL slurry of either silica or immunoaffinity beads to the top of the column body tubing drop-wise. A jewelry engraver was used to periodically vibrate the sides of the column during packing to remove air pockets. When the beads were observed at the top of the column, the assembly was removed and the open end covered with Parafilm. The column was then gently tapped on the bench top and inspected under magnification. The procedure was repeated until the stationary phase persisted at the column head. Next, the top of the column was leveled with a stainless steel spatula and the end fitting containing the second frit was gently reassembled. Column lengths of 25 and 50 mm were packed by this procedure and tested as prototype separation columns.

2.4. Software design

Two software programs were designed for instrument control/data acquisition and data analysis using LabVIEW (National Instruments). For the control/acquisition program, the dual microliter syringe pumps were connected through computer serial ports and run simultaneously. The pump user's manual

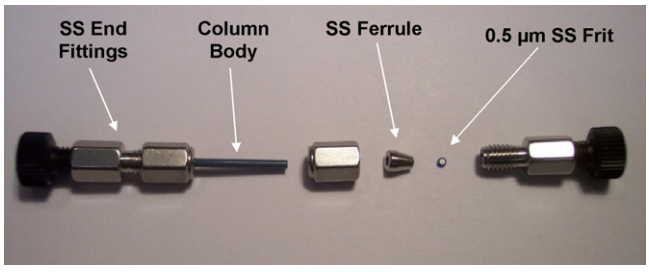

Fig. 2. Components of the prototype capillary column. The column body is made of polymer-coated fused-silica and all fitting are stainless steel (SS).

specified the serial port connection inputs and language commands through HyperTerminal control in Windows-based computers. These commands and connections form the basis for controlling the dual pumping system in LabVIEW. The syringe volume and diameter were defined along with all computer addresses connected to the pumps and detector. A timed events window was created to allow for changes in flow rate to be input for each pump for a desired duration of time. There are a total of 20 lines of input, corresponding to 20 possible lines of gradient programming. After a defined time duration in line one, the data acquisition begins and the LIF signal is displayed as a real time chromatogram from the USB card interface. Manual injections are made at the end of line one to improve reproducibility. Each running of the program requires a file path, where the chromatogram is stored.

The file can be recalled in the data analysis program which regenerates the chromatogram and relies on user-input threshold values to define a reportable peak. The software requires confirmation of a selected peak and then imports the peak into a window where integration is performed. Both area under the curve and height are reported. In LabVIEW, the front panel screen is part of a virtual instrument with user input fields and functions such as on/off switches and LED's. The actual programming is contained in a second screen called a block diagram. A portion of the front panel screen for the control/acquisition program is shown in Fig. 3.

2.5. System optimization

Two prototype columns were packed with 1 μm silica spherical particles and evaluated with respect to measurement of flow rate accuracy. In order to confirm the flow rate water was pumped through each column for 10 min at 1.0 μL/min, collected in a 200 μL polypropylene tube, and measured with Hamilton glass syringes. Each column had an inner diameter of 200 μm and lengths of either 25 or 50 mm. Additionally, Nucleosil 10 μm C8 particles (Alltech, Deerfield, IL) were packed into a 200 μm by 50 mm column. All tests were performed in triplicate.

Evaluation of the system mixer was performed by programming a step gradient of pH 7.4, 100 mM phosphate in pump A and 800 pM Alexa Fluor 647 in pH 7.4, 100 mM phosphate for pump B. Observed profiles, in triplicate, were compared to the programmed gradient profile. The plateau of each step was measured and plotted versus concentration.

The ability of the pumps and mixer to perform a pH gradient was tested by measuring the pH of column effluent after a linear acidic gradient program was run. Pump A contained pH 7.4 100 mM phosphate and pump B contained a pH 1.2 glycine–HCl solution. Offline measurements of premixed solutions were compared to online measurements at the same proportions using the mixer. Offline measurements were made with an Orion model

Fig. 3. Control and acquisition front panel. This screen allows pump control, gradient programming, and data acquisition settings of duration and sampling rate. The chromatogram is viewed in real time. The first 10 lines of gradient input are shown.

920A+ pH meter (Thermo Electron Corporation, Waltham, MA) and online measurements were made with pH paper indicators (Micro Essential Laboratory, Brooklyn, NY).

Various concentrations of Alexa Fluor 647 laser dye were prepared in water and injected into the system to evaluate the detector system. A calibration curve was tested in triplicate at concentrations of 100, 200, 400, 600, and 800 pM and a linear regression was used to obtain an equation for the line. A blank was injected $n = 3$ times and the peak-to-peak noise was measured across the elution window of the dye peak. The limit of detection (LOD) was calculated by the equation $\mathrm{LOD} = 3S_b/m$, where S_b is the standard deviation of the blank peak-to-peak noise and m is the slope from the calibration curve.

2.6. IgG immunoaffinity chromatography as proof-of-principle

Goat IgG was used as a model antigen and rabbit anti-goat IgG was used as the immobilized capture antibody. Streptavidin-coated glass beads and biotinylated rabbit anti-goat IgG were combined in a ratio of 3 mg: 150 ng in 1 mL of 10 mM phosphate buffer pH 7.2. The mixture was placed onto a rotary mixer for 1 h at room temperature and 15 h at 4 °C. The particles were washed three times in 10 mM phosphate buffer, pH 7.2 and incubated with 50 ng/mL of biotin at 4 °C for 2 h. The particles were then washed five times and reconstituted in 10 mM phosphate buffer pH 7.2. The activity of the immunoaffinity stationary support was tested by placing 300 μg of particles and 7.5 ng of Alexa Fluor 647-labeled goat IgG on a rotary mixer for 2 h at room temperature. Three replicates were prepared along with three controls of Alexa Fluor 647 without the immunoaffinity glass particles. The solution was centrifuged at 1200 rpm for 10 min and the supernatant was injected into the flow cell of the LIF detector. The stationary phase was found to remove approximately 79% of the Alexa Fluor 647-goat IgG from solution versus controls.

A 0.2 mm × 25 mm capillary column was packed with the immunoaffinity stationary phase as described above and stored at 4 °C until use. Solutions of Alexa Fluor 647-goat IgG were prepared in 10 mM phosphate, pH 7.2 at 111, 333, 667, and 1000 pM. After injection of the antigen, a 10 mM phosphate buffer solution was applied for 4 min, followed by a linear elution gradient of 2.5 M sodium thiocyanate. The column was then equilibrated with 10 mM phosphate buffer. The flow rate was 1.5 μL/min and the column was kept in an ice water jacket while running samples.

3. Results and discussion

In the present work, we have combined two syringe pumps with a nano-gradient mixing chip for the production of gradients with capillary-scale tubing and separation columns. The OEM module microliter syringe pumps are capable of providing a wide range of flow rates from 0.0001 to 791.8 μL/min using syringe sizes from 1 to 1000 μL. Simple serial commands for the RS-232 interface with HyperTerminal control in Windows-based computers can be used to run the pumps and change flow rates with no additional software requirements. For automated gradients, a custom program has been written in LabVIEW software that varies the flow rate of each pump over timed steps. The gradient mixing chip was demonstrated to produce adequate mixing for gradients of fluorescent dye and pH changes.

The column assembly is straightforward to construct and flexible in design. The material, inner diameter, and length of tubing can be changed to create a variety of dimensions for multiple applications. The column packing procedure using a vacuum pump is both gentle and efficient, making it suitable for immunoaffinity and other fragile stationary phases. A similar packing procedure has been reported by Qu et al. [33] for use with capillary electrochromatography with the noted advantage uncomplicated assembly and operation. The syringe pumps, nano-gradient mixer, micro-injector, and capillary column components presented here are all commercially available and relatively simple to construct into a functional chromatography system.

The operational capabilities and limitations of the pumps were determined by the manufacturer specifications for the syringes and syringe pumps. Table 1 was created using the nominal syringe pump force in pounds and syringe internal diameter in square inches. Dividing the pump force by the syringe internal diameter gives maximum operational pressure ratings in pounds per square inch (psi). The operational pressure rating of syringes and pumps increases with decreasing syringe size. For example, changing from a 500 to a 100 μL syringe increases the pump pressure capacity from approximately 500 psi to greater than 2000 psi. The 100 μL syringe is only rated up to 1000 psi. The syringe size and corresponding pressure rating are limiting factors for the determination of an overall system pressure threshold. Another important consideration for use with immunoaffinity stationary phases is that such supports can start to degrade at pressures higher than 500 psi [34].

A prototype column was selected by measuring flow rate accuracy while varying particle size and column length. Water

Table 1
Syringe and pump pressure with syringe size

Syringe	Syringe size (μL)	Max. syringe pressure (psi)[a]	Syringe internal diameter (in.^{2})[a]	Max. pump pressure (psi)
Hamilton glass gastight	500	500	0.012938	464
	100	1000	0.002595	2312

The Harvard Apparatus microliter syringe pump delivers 6 pounds of force.

[a] Data from Harvard Apparatus website for Hamilton 1700 series Gastight syringes (http://www.harvardapparatus.com/).

Table 2
Flow rate accuracy with respect to syringe size, column length, and particle size changes

Column	Syringe size (μL)	Average measured volume (μL)
0.2 mm × 50 mm, 1 μm silica	500	7.0 ± 0.6
0.2 mm × 50 mm, 1 μm silica	100	9.9 ± 0.4
0.2 mm × 25 mm, 1 μm silica	500	10.0 ± 0.0
0.2 mm × 50 mm, 10 μm C_8	500	10.0 ± 0.3

Mobile phase: water, flow rate: 1.0 μL/min, duration: 10 min, expected volume: 10 μL, 3 replicates.

pumped at a flow rate of 1.0 μL/min was chosen for all columns for the sake of uniformity. Both a 100 and a 500 μL syringe were used to evaluate flow rate accuracy through the prototype columns. Packing the capillaries with 1 μm beads took approximately 2 h for the 25 mm column and 6–7 h for the 50 mm column. Results of the flow rate accuracy evaluation are shown in Table 2. The 50 mm column packed with 1 μm silica delivered a volume of pumped water that was 30 ± 6% less than expected when using a 500 μL syringe. When the same column was reevaluated using a 100 μL syringe, the accuracy improved to 99 ± 4% of the expected volume. It was concluded that the maximum pressure rating of the 500 μL syringe (500 psi) may have been exceeded with this column. Leakage around the plunger of the 500 μL syringe was observed, indicating syringe failure as the source of flow rate inaccuracy. A 25 mm prototype column packed with 1 μm beads was also evaluated. The volume delivered was as expected when using a 500 μL syringe (10.0 ± 0.0 μL) and no leakage was observed. The 25 mm prototype column was therefore chosen to perform further optimization studies of the instrument. This column allows for the use of the larger (500 μL) syringe, which effectively increases the amount of mobile phase that can be loaded onto the pumps without refilling a syringe during sample analysis. Further optimization of the system was carried out with the 25 mm prototype and 50 mm column packed with 10 μm C8 particles was also examined. The larger particle size allowed for the use of both the longer column and larger syringe (500 μL), while maintaining flow rate accuracy. These findings agree with the expected relationship between pressure and an HPLC column packed with spherical particles. Pressure is approximately proportional to column length, but inversely proportional to the particle diameter squared [35].

A mixing profile was created by measuring the Alexa Fluor 647 dye signal at different programmed proportions pumped through the 0.2 mm × 25 mm column packed with 1 μm silica beads (Fig. 4A and B). Pump B contained the dye and was programmed from a starting proportion of 2.5% up to 97.5% in a four step gradient. At 1.5 μL/min there was approximately 3 min of lag time between the observed signal and programmed mixing. The height above baseline for the plateau at each step was plotted against the concentration of dye being pumped (Fig. 4C). The line was fit with a linear regression and an R^2 value of 0.9998 was obtained.

Gradient accuracy was further confirmed by monitoring pH changes through the 0.2 mm × 25 mm column. A neutral

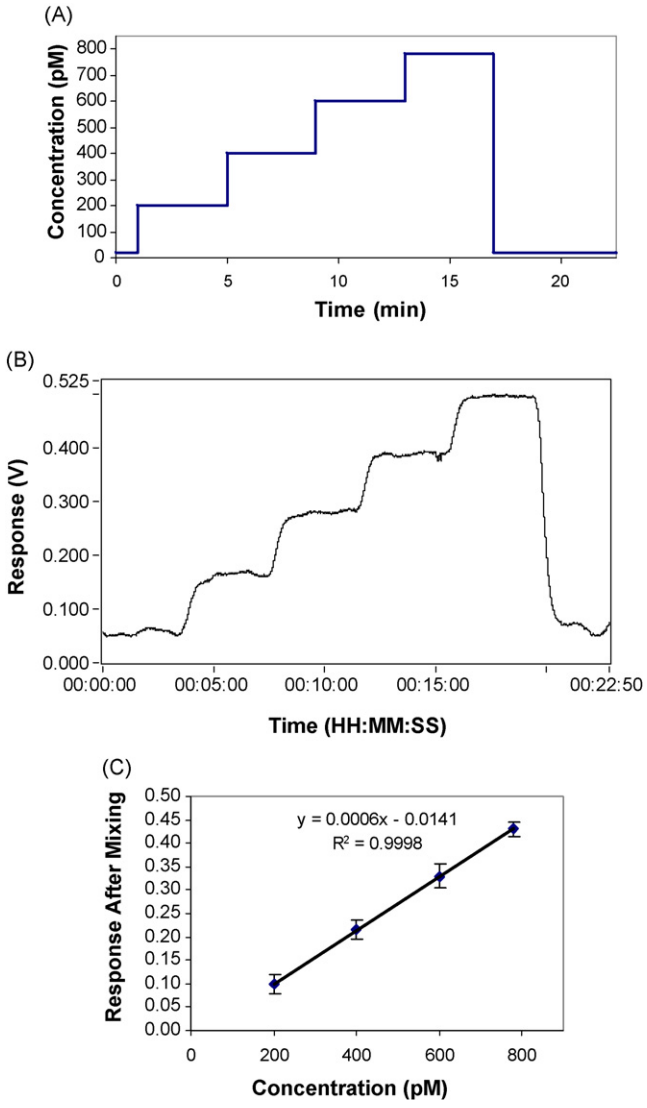

Fig. 4. Programmed (A) and observed detector response (B) of a step gradient using Alexa Fluor 647 dye. Pump A contained 100 mM phosphate buffer pH 7.4 and pump B contained 1000 pg/mL Alexa Fluor 647 dye in 100 mM phosphate buffer pH 7.4. Flow rate was 1.5 μL/min. The plateau of each step was plotted vs. the concentration of dye pumped for $n = 3$ replicates (C). Error bars represent one standard deviation.

phosphate to acidic glycine–HCl gradient was programmed at 1.0 μL/min using the software. Column effluent was spotted on pH paper every 30 s and only visually clear, whole pH unit changes were recorded. The observed pH was plotted versus time and overlaid with the programmed acidic gradient (Fig. 5). The observed profile indicated that the system was capable of producing an acid gradient suitable for immunoaffinity elution. The delay in observed pH change versus programmed pH gradient can be attributed to the system dwell volume. The stagnation in pH between minutes 8 and 10 is due to limitations of measuring observed pH using pH paper in whole units. Fixed proportions of pump A to pump B buffers were measured online with pH paper and offline with a pH meter at 30, 35, and 50% glycine–HCl. For the 30, 35, and 50% pH 1.2 glycine–HCl solutions, the pH meter readings were 6.0, 5.8, and 2.6, respectively. The corresponding

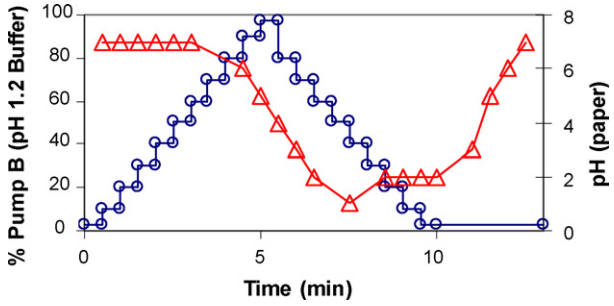

Fig. 5. Ability of the system to produce an acid gradient. The line with open circles represents a gradient of Pump B programmed in LabVIEW. The open triangles represent the observed pH values in whole units. Conditions described in text.

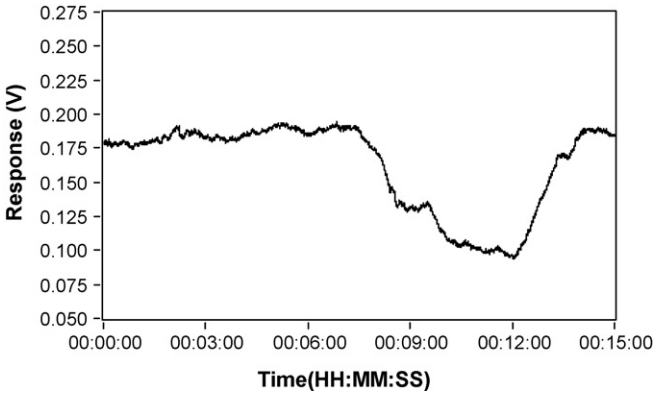

Fig. 6. Baseline change after injection of a blank 10 mM phosphate buffer. Run conditions are as described in the text.

post-column measurements with pH paper were 6, 6, and 3, and were limited to whole unit readings.

Aqueous solutions of Alexa Fluor 647 dye were injected onto the 0.2 mm × 25 mm column at 1.5 μL/min in a mobile phase consisting of unbuffered water to determine the detection limit of the system. Injection loops of 750 nL, 1.0 μL, and 1.6 μL were evaluated and a 1.0 μL injection loop was chosen for sample introduction. Peak intensity and shape were optimal with the 1.0 μL loop. A linear regression fit of the data resulted in a R^2 value of 0.9918. The LOD, calculated as three times the standard deviation of the blank divided by the slope of the calibration curve, was determined to be 10 pM or 10 amol on column.

The ability of a system to detect low picomolar concentrations of laser dye-labeled proteins is attractive for clinical applications. The demonstrated low detection limit of dye solutions shows promise in this regard and may be improved further since immunoaffinity chromatography allows online sample concentration. For example, Guzman has developed a solid-phase microdevice capable of concentrating samples 1000-fold online with immunoaffinity capillary electrophoresis [4]. Other factors may be changed to further improve the detection limit of the system. In the current microfluidic instrument, the post-column capillary used for the flow cell is 100 μm inner diameter. Reducing this capillary to 75 or 50 μm inner diameter would reduce extra-column peak spreading, resulting in lower limits of detection. The maximum flow rate achieved without exceeding the pressure capacity of the syringe was 1.5 μL/min. Increasing the flow rate would also help improve peak shape, but was not an option for the 0.2 mm × 25 mm prototype column packed with 1 μm silica beads due to exceeding the pressure rating for the syringes. Alternatively, the use of larger particle sizes for column packing material would allow for faster flow rates with this system, but also will lead to peak broadening.

To demonstrate that the system was suitable for immunoaffinity chromatography, a 0.2 mm × 25 mm prototype column was packed with 5.7 μm glass particles coated with rabbit anti-goat polyclonal antibodies. Alexa Fluor 647-goat IgG solutions were injected into the microfluidic system using a 1.0 μL injection loop. Introduction of a sodium thiocyanate gradient had a pronounced effect on the baseline, as is shown for an injection of blank phosphate buffer (Fig. 6). The signal decreases as the chaotropic gradient is introduced and rises as the mobile phase returns to the starting phosphate buffer. The reason for the baseline drop with 2.5 M sodium thiocyanate is not known, but may be due to a quenching phenomenon or refractive index change. Chromatograms of goat IgG-fluorescent dye solutions show a large first peak of unbound material and a second peak corresponding to captured antigen. Fig. 7 shows a representative chromatogram of goat IgG at 667 pM with the immunoaffinity-purified peak eluting just before the baseline dip induced by the gradient. This chromatogram was the 25th overall injection on the column. A linear regression resulted in a slope of 0.0858 and an R^2 value of 0.9963 using peak areas and concentrations from 111 to 1000 pM. Further optimization of this proof-of-principle model will focus on maximizing antigen recovery and minimizing the baseline effect of the chaotropic gradient. Antigen recovery may be improved by varying loading or running buffer conditions. The pH and/or salt concentration of the running buffer will have an effect on the degree of antibody–antigen binding. Instrumental parameters such as flow rate may be varied as well. An optimized flow rate would utilize the fastest runtime that still provided time for the antibody–antigen reaction to occur. The baseline effect can be minimized by using the lowest effective concentration the chaotropic buffer or changing to a different type of elution buffer, for example acidic elution. The column was maintained at 15 °C and an approximately 40%

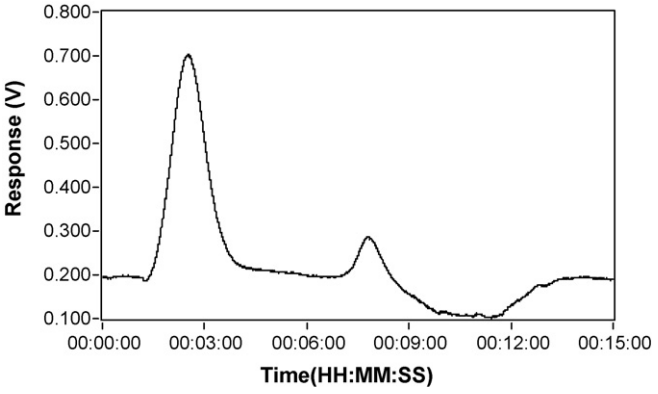

Fig. 7. Representative immunoaffinity chromatogram of goat IgG labeled with Alexa Fluor 647 dye. The first peak is the unbound material and the second peak is immunoaffinity purified goat IgG. Conditions are described in the text.

decrease in antigen binding capacity was observed gradually between 40 and 50 injections. A new ice water jacket has been constructed from copper tubing that maintains column temperature at 5 °C and it is expected to help increase column lifetime. A peristaltic pump is used to pump ice water through a copper coil wrapped around the separation column.

4. Conclusions

A laboratory-constructed capillary HPLC with visible diode laser-induced fluorescence detection is presented. Separation columns were designed and optimized with respect to syringe size, column length, and particle size. The prototype column chosen for proof-of-concept testing was a 200 μm × 25 mm polymer-coated fused-silica capillary. The ability of the microliter syringe pumps and nano gradient mixer chip to perform as a microfluidic gradient HPLC has been demonstrated through a series of programmed evaluations. Pumping software-programmed amounts of fluorescent dye through the mixer created response profiles that correlated well with expected concentration increases. Furthermore, an acidic gradient was confirmed by pH readings of column effluent and offline measurements. Throughout the optimization, the software programs were verified by accurately controlling the components to function as a miniaturized chromatography system.

Effective immunoaffinity chromatography requires an elution scheme and instrumentation capable of producing gradients that dissociate the antibody–antigen complex. The system constructed meets this need and requires low amounts of reagents and samples, which can be an advantage when working with expensive immuno-reagents or when rapid results are needed. A goal for the instrument was to reach limits of detection in the low picomolar range. The system was developed in response to the need for rapid and selective assays including intraoperative assays and point-of-surgery tests, or other point-of-care applications. Many of the intraoperative assays, such as parathyroid hormone testing for example, require measuring baseline levels at low picomolar concentrations [36,37]. A LOD of 10 pM was obtained for neat solutions of Alexa Fluor 647 with the prototype instrument. Online sample concentration can be achieved using immunoaffinity chromatography by loading relatively large injection volumes onto the column for antigen capture by an immobilized antibody support. The sample antigen can then be released from the column in a volume that is smaller than the injected volume for enhanced detection.

Immunoaffinity chromatography was demonstrated using immobilized rabbit anti-goat IgG and fluorescently labeled goat IgG as a model antibody–antigen system. The immunoaffinity stationary phase was comprised of antibody attached to glass beads via a streptavidin–biotin linkage. A chaotropic gradient was chosen for antigen elution and a concentration-dependent increase in fluorescence signal was observed. The flow rate, injection volume, and elution scheme are currently under evaluation to optimize the antigen capture and release onto and off of the column. The device presented was laboratory-built from a combination of commercially available materials. The relatively simple construction and compact nature of instrument components may be advantageous in clinical and research settings where system flexibility and portability are desired.

References

[1] P. von Lode, Clin. Biochem. 38 (2005) 591.
[2] M.C. Hennion, V. Pichon, J. Chromatogr. A 1000 (2003) 29.
[3] Z. Tang, H.T. Karnes, Biomed. Chromatogr. 14 (2000) 442.
[4] N.A. Guzman, Electrophoresis 24 (2003) 3718.
[5] P. Su, X.X. Zhang, W.B. Chang, J. Chromatogr. B Analyt. Technol. Biomed. Life Sci. 816 (2005) 7.
[6] S.B. Cheng, C.D. Skinner, J. Taylor, S. Attiya, W.E. Lee, G. Picelli, D.J. Harrison, Anal. Chem. 73 (2001) 1472.
[7] J. Wang, A. Ibanez, M.P. Chatrathi, A. Escarpa, Anal. Chem. 73 (2001) 5323.
[8] K. Sato, M. Tokeshi, H. Kimura, T. Kitamori, Anal. Chem. 73 (2001) 1213.
[9] N.H. Chiem, D.J. Harrison, Clin. Chem. 44 (1998) 591.
[10] M. Wolf, D. Juncker, B. Michel, P. Hunziker, E. Delamarche, Biosens. Bioelectron. 19 (2004) 1193.
[11] T.M. Phillips, E. Wellner, J. Chromatogr. A (2006).
[12] T.M. Phillips, Electrophoresis 25 (2004) 1652.
[13] Y. Murakami, T. Endo, S. Yamamura, N. Nagatani, Y. Takamura, E. Tamiya, Anal. Biochem. 334 (2004) 111.
[14] A. Dodge, K. Fluri, E. Verpoorte, N.F. de Rooij, Anal. Chem. 73 (2001) 3400.
[15] M. Jia, Z. He, W. Jin, J. Chromatogr. A 966 (2002) 1857.
[16] T.M. Phillips, Anal. Chim. Acta 372 (1998) 209.
[17] T.K. Lim, T. Matsunaga, Biosens. Bioelectron. 16 (2001) 1063.
[18] T.M. Phillips, P.D. Smith, J. Liquid Chromatogr. Related Technol. 25 (2002) 2889.
[19] M.A. Hayes, T.N. Polson, A.N. Phayre, A.A. Garcia, Anal. Chem. 73 (2001) 5896.
[20] D.S. Hage, J. Chromatogr. B Biomed. Sci. Appl. 715 (1998) 3.
[21] M.G. Weller, Fresenius, J. Anal. Chem. 366 (2000) 635.
[22] N.A. Guzman, R.J. Stubbs, Electrophoresis 22 (2001) 3602.
[23] N.A. Guzman, T.M. Phillips, Anal. Chem. 77 (2005) 61A.
[24] W.S.B. Yeung, G.A. Luo, Q.G. Wang, J.P. Ou, J. Chromatogr. B 797 (2003) 217.
[25] L.B. Bangs, Pure Appl. Chem. 68 (1996) 1873.
[26] E. Verpoorte, Lab. Chip 3 (2003) 60N.
[27] T. Buranda, J. Huang, V.H. Perez-Luna, B. Schreyer, L.A. Sklar, G.P. Lopez, Anal. Chem. 74 (2002) 1149.
[28] R.J. Hodgson, M.A. Brook, J.D. Brennan, Anal. Chem. 77 (2005) 4404.
[29] T. Jiang, R. Mallik, D.S. Hage, Anal. Chem. 77 (2005) 2362.
[30] A. Ducret, N. Bartone, P.A. Haynes, A. Blanchard, R. Aebersold, Anal. Biochem. 265 (1998) 129.
[31] A. Cappiello, G. Famiglini, C. Fiorucci, F. Mangani, P. Palma, A. Siviero, Anal. Chem. 75 (2003) 1173.
[32] J. Zhou, F. Rusnak, T. Colonius, G.M. Hathaway, Rapid Commun. Mass Spectrom. 14 (2000) 432.
[33] Q. Qu, X. Hu, X. Zhu, S. Gao, Q. Xu, Y. Wang, X. Wang, J. Sep. Sci. 27 (2004) 1229.
[34] T.M. Phillips, B.F. Dickens, Affinity and Immnuoaffinity Purification Techniques, Eaton Publishing, Natick, MA, 2000.
[35] L.R. Snyder, J.J. Kirkland, J.L. Glajch, Practical HPLC Method Development, John Wiley & Sons Inc., New York, 1997.
[36] M. Friedman, R. Vidyasagar, D. Bliznikas, N.J. Joseph, Laryngoscope 115 (2005) 34.
[37] N.R. Vasan, K.E. Blick, G.A. Krempl, J.E. Medina, Otolaryngol. Head Neck Surg. 131 (2004) 610.